

# A Large $\pi$ -Extended Carbon Nanoring Based on Nanographene Units: Bottom-Up Synthesis, Photophysical Properties, and Selective Complexation with Fullerene C<sub>70</sub>

Dapeng Lu<sup>+</sup>, Guilin Zhuang<sup>+</sup>, Haotian Wu, Song Wang, Shangfeng Yang, and Pingwu Du\*

**Abstract:** Herein we report the organoplatinum-mediated bottom-up synthesis, characterization, and properties of a novel large  $\pi$ -extended carbon nanoring based on a nanographene hexa-*peri*-hexabenzocoronene (HBC) building unit. This tubular structure can be considered as an example of the longitudinal extension of the cycloparaphenylene scaffold to form a large  $\pi$ -extended carbon nanotube (CNT) segment. The cyclic tetramer of a tetramesityl HBC ([4]CHBC) was synthesized by the reaction of a 2,11-diborylated hexa-*peri*-hexabenzocoronene with a platinum complex, followed by reductive elimination. The structure of this tubular molecule was further confirmed by physical characterization. Theoretical calculations indicate that the strain energy of this nanoring is as high as 49.18 kcal mol<sup>-1</sup>. The selective supramolecular host–guest interaction between [4]CHBC and C<sub>70</sub> was also investigated.

Carbon nanotubes (CNTs) with a specific diameter and chirality are important in nanotechnology and nanoelectronics. The synthesis of length- and diameter-specific CNT segments is a challenge in organic synthesis and materials science. Surface-mediated strategies have shown great promise for the preparation of structurally uniform CNTs, such as the recently reported growth of CNTs on a platinum surface<sup>[1]</sup> or on solid alloy catalysts,<sup>[2]</sup> and the longitudinal growth of cycloparaphenylene (CPP) precursors.<sup>[3]</sup> Regarding precise structural control, the solution-processable bottom-up approach is another desirable strategy to produce pure CNTs. CPPs have hoop-shaped structures consisting of aromatic rings with *para* linkages and are the shortest conjugated fragment of armchair nanotubes, which have been proposed as ideal precursors for the bottom-up synthesis of structurally uniform CNTs.<sup>[3,4]</sup> Initial synthetic endeavors targeting CPPs were reported by Parekh and Guha in 1934.<sup>[5]</sup> Modern CPP research can be traced back to a report by

Vögtle and co-workers, in which they suggested several ingenious strategies for the synthesis of CPPs,<sup>[6]</sup> which led to the successful synthesis of a picotube in 1996.<sup>[7]</sup> The initial synthesis of [9]-, [12]-, and [18]CPPs from a curved precursor was reported in 2008,<sup>[8]</sup> and several other strategies involving curved linkers or platinum-mediated catalysis have also been explored for the production of CPPs.<sup>[4a,9]</sup>

Further  $\pi$  extension of the CPP system was recently reported. The incorporation of naphthalene,<sup>[10]</sup> chrysene,<sup>[11]</sup> and pyrene<sup>[12]</sup> building blocks into the carbon nano-hoops are representative examples. In view of the difficulty in functionalizing the building blocks to create a fully  $\pi$ -conjugated CNT sidewall segment, large conjugated systems could also be formed by using a postconstruction method, such as a cyclo-dehydrogenation reaction after the formation of the cyclic structure.<sup>[13]</sup> Our research group recently introduced two HBC units as sidewalls into the [18]CPP backbone by palladium-catalyzed Suzuki coupling.<sup>[14]</sup>

Despite all of the above progress, a large  $\pi$ -extended carbon nanoring containing only HBC units has only been detected by mass spectroscopy,<sup>[13b]</sup> but no isolated pure product has been reported so far. Such a cyclic structure consisting solely of HBC units more closely resembles a CNT segment than previously reported carbon nanorings<sup>[8,9]</sup> and could be a good precursor for the bottom-up synthesis of uniform CNTs. Therefore, the synthesis of such a structure and evaluation of its electronic properties is highly desired.

Herein we report the synthesis and isolation of a large  $\pi$ -extended carbon nanoring as a finite model of CNTs based on four HBC units, [4]cyclo-2,11-*para*-hexa-*peri*-hexabenzocoronene ([4]CHBC, Figure 1). A platinum-mediated assembly approach was used, followed by a reductive-elimination reaction. Platinum-mediated synthesis is a useful method for the construction of conjugated structures by the assembly of

[\*] D. Lu,<sup>[†]</sup> H. Wu, S. Wang, Prof. S. Yang, Prof. P. Du  
CAS Key Laboratory of Materials for Energy Conversion  
Department of Materials Science and Engineering, Collaborative  
Innovation Center of Chemistry for Energy Materials (iChEM)  
University of Science and Technology of China (USTC)  
Hefei, 230026 (P.R. China)  
E-mail: dupingwu@ustc.edu.cn  
Prof. G. Zhuang<sup>[†]</sup>  
College of Chemical Engineering, Zhejiang University of Technology  
18, Chaowang Road, Hangzhou, Zhejiang Province 310032 (China)

[†] These authors contributed equally.

Supporting information and the ORCID identification number(s) for the author(s) of this article can be found under <http://dx.doi.org/10.1002/anie.201608963>.

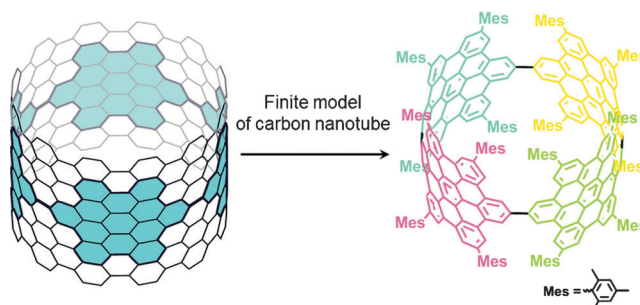


**Figure 1.** Design of the tubular [4]CHBC carbon nanoring as a finite model of a carbon nanotube.

$\pi$ -conjugated units and subsequent carbon–carbon bond formation by reductive elimination.<sup>[9a,15]</sup>

The HBC unit with tetramesityl groups is a good building block because of its high solubility in common organic solvents. Mesityl groups can be introduced at the HBC periphery by the coupling of tetrabromohexaphenylbenzene with mesitylmagnesium bromide, followed by cyclodehydrogenation with  $\text{FeCl}_3$ . This tetramesityl-substituted HBC was subsequently converted into the 2,11-diborylated tetramesityl HBC **1** (Figure 2) by treatment with an equimolar amount of bis(pinacolato)diboron under iridium(I)-catalyzed borylation conditions.<sup>[16]</sup> This convenient protocol for the introduction of boryl groups into  $\pi$ -rich hydrocarbons through direct C–H borylation provides a reliable method for the preparation of large quantities of *para*-borylated tetramesityl HBC, which is a key precursor for the synthesis of [4]CHBC.

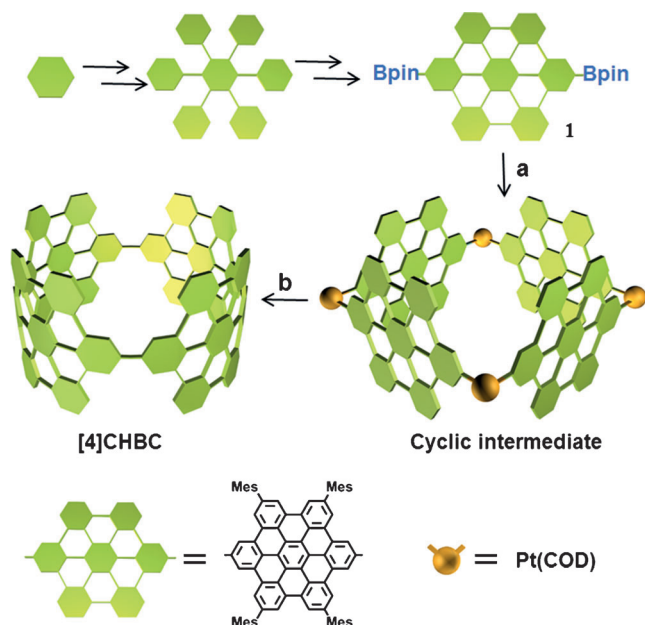


**Figure 2.** Synthetic strategy for [4]CHBC. a) CsF (6.0 equiv),  $[\text{Pt}(\text{cod})\text{Cl}_2]$  (1.1 equiv), THF, reflux, 24 h; b) platinum-mediated reductive elimination: triphenylphosphine (10 equiv), mesitylene, 150 °C. COD = 1,5-cyclooctadiene.

Next, the macrocyclization reaction was performed by the platinum-mediated cyclization method.<sup>[17]</sup> In the presence of cesium fluoride, the HBC precursor **1** reacted with an equimolar amount of  $[\text{Pt}(\text{COD})\text{Cl}_2]$  in dry THF under reflux. The resulting mixture was directly subjected to reductive elimination by heating in the presence of triphenylphosphine (10 equiv) in dry mesitylene for 48 h under nitrogen (Figure 2). After extensive purification by initial flash column chromatography and then preparative thin-layer chromatography, the target nanoring molecule [4]CHBC was obtained as a yellow solid in 5.4% yield over two steps, which is comparable to the yields of many similar reactions.<sup>[17a,18]</sup> Although other cyclic oligomers with more than four HBC units (such as [5]CHBC) could also be produced, it would be very difficult to characterize them owing to their much lower

yields. We have also attempted to optimize the reaction conditions to improve the ultimate yield of our product by adjusting the solvent, temperature, and base, but no further improvement was observed in the yield of [4]CHBC.

The molecular weight of [4]CHBC was determined by MALDI-TOF MS spectrometry. A main peak at  $m/z$  3973.96 was observed (calculated for  $\text{C}_{312}\text{H}_{225} [\text{M}+\text{H}]^+$ : 3973.79), thus suggesting the synthesis of the target molecule (Figure 3 a). The  $^1\text{H}$  NMR spectrum of [4]CHBC featured a set of signals

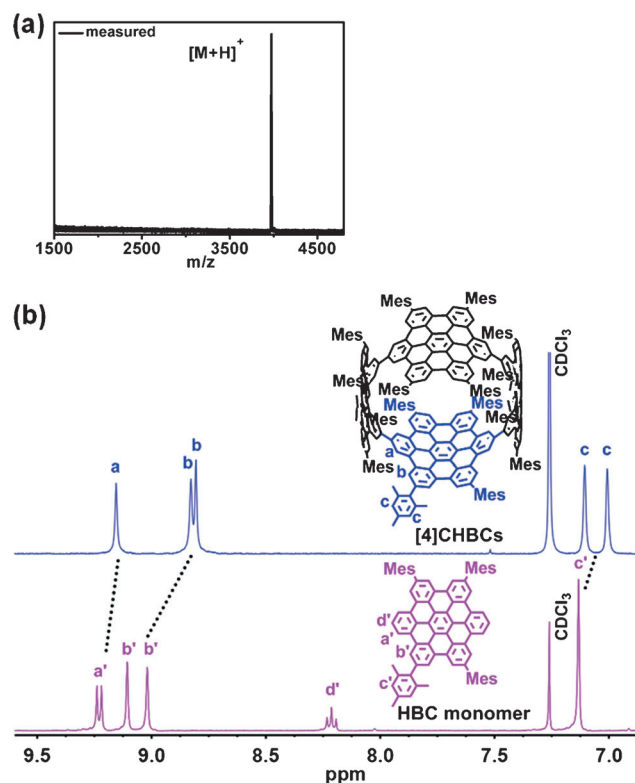


**Figure 3.** a) MALDI-TOF MS of [4]CHBC. b) Comparison of the aromatic regions of the  $^1\text{H}$  NMR spectra of [4]CHBC and the tetramesityl HBC monomer.

with the signature of only seven singlets, thus indicating its highly symmetric structure (see the Supporting Information). Figure 3 b shows a comparison of proton signal patterns in the aromatic region between [4]CHBC and the tetramesityl HBC monomer. Clear splitting of peaks as a result of spin–spin coupling between adjacent proton(s) can be observed in the spectrum of the monomer (peaks a' and d' in Figure 3 b). In sharp contrast, these coupling peaks disappear for [4]CHBC, thus indicating that the HBC units are connected to form a hoop-shaped and highly symmetric structure. Another distinct feature is that the signals of the hydrogen atoms at the peripheries of [4]CHBC are shifted upfield as compared to the corresponding peaks of the monomer, thus indicating the influence of adjacent HBC units in the nanoring structure. The  $^1\text{H}$  and  $^{13}\text{C}$  NMR data and UV absorption and emission spectra (see below) confirmed the successful synthesis of [4]CHBC.

The photophysical properties of [4]CHBC were studied by UV/Vis absorption spectroscopy, steady-state fluorescence spectroscopy, and time-resolved fluorescence decay. The tetramesityl HBC monomer was used as a reference compound for comparison. The absorption bands of [4]CHBC were observed between 300 and 500 nm, and the maximum absorption peak ( $\lambda_{\text{max}}$ ) was observed at 375 nm with the molecular absorption coefficient  $\epsilon = 5.1 \times 10^5 \text{ cm}^{-1} \text{ M}^{-1}$  (Figure 4a). Two moderate absorption peaks were also observed with maxima at 431 and 458 nm. Notably, the absorption feature of [4]CHBC showed a clear redshift in comparison with those for the tetramesityl HBC and other CPPs.<sup>[19]</sup> This redshift could be ascribed to the larger  $\pi$ -conjugation system from the HBC units and the cyclic structure.

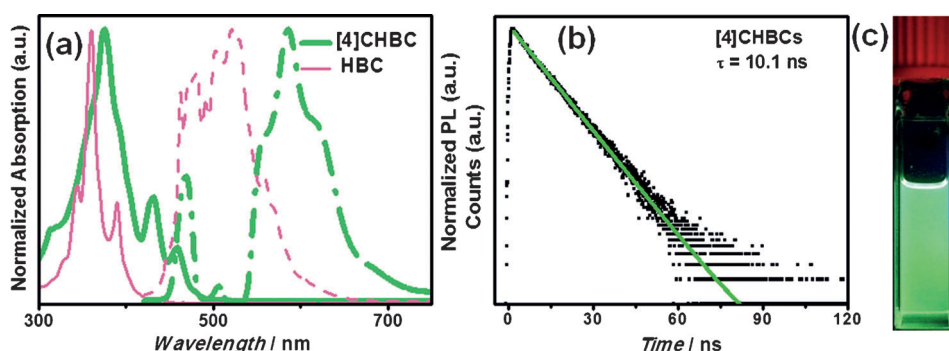


**Figure 4.** a) UV/Vis absorption (solid lines) and fluorescence spectra (dash lines) of [4]CHBC (green) and tetramesityl HBC (pink) in  $\text{CH}_2\text{Cl}_2$ . b) Emission lifetime measured at 585 nm for [4]CHBC in  $\text{CH}_2\text{Cl}_2$ . c) Photograph showing the fluorescence of [4]CHBC in  $\text{CH}_2\text{Cl}_2$  under a UV lamp. PL = photoluminescence.

The emission spectrum of [4]CHBC showed multiple emission bands with maximum peaks at 468, 506, and 586 nm ( $\lambda_{\text{ex}} = 400 \text{ nm}$ ). The edge emission was even extended to 750 nm. Similarly, these emission bands were significantly shifted towards lower energy as compared with the emission spectrum of the monomer, which is consistent with the UV/Vis result and confirms the  $\pi$ -expanded nature in [4]CHBC. This solution also presented an intense greenish photoluminescence under irradiation by a hand-held UV lamp (Figure 4c).<sup>[20]</sup> The photoluminescence quantum yield was determined to be  $\Phi_{\text{F}} = 8.3\%$  by using anthracene as the reference ( $\Phi_{\text{F}} = 30\%$  in ethanol). This value is lower than those of tetramesityl HBC and CPPs (for tetramesityl HBC,  $\Phi_{\text{F}} = 14.8\%$ , and for [9]–[16]CPP, the  $\Phi_{\text{F}}$  values range from 73 to 88%),<sup>[19]</sup> probably as a result of the high proportion of nonradiative decay in the low-energy emission.

Upon excitation at 390 nm, the luminescence lifetime ( $\tau_{\text{s}}$ ) of [4]CHBC was determined to be approximately 10.1 ns at 585 nm by single-exponential decay fitting (Figure 4b). As for the tetramesityl HBC, a similar single-exponential decay was observed with  $\tau_{\text{s}} \approx 18.0 \text{ ns}$  at 520 nm at the same excitation wavelength (see Figure S1 in the Supporting Information). The fluorescence lifetime of [4]CHBC is longer than that of [12]CPP ( $\tau_{\text{s}} = 2.2 \text{ ns}$ ).<sup>[19]</sup>

To investigate the structure and electronic properties of the nanoring [4]CHBC, we performed density functional

theory (DFT) calculations with the DMol<sup>3</sup> software.<sup>[21]</sup> For simplification, we replaced all the peripheral methyl groups with hydrogen atoms in the initial geometrical optimization owing their negligible influence on the conjugated framework of this structure (Figures 5a,b). The structure features  $D_2$  symmetry with all atoms relaxed without constraints. Each HBC monomer is linked to adjacent monomers by a C–C single bond of about 1.485 Å in length with a torsion angle of approximately 35.98°. Inspecting the frontier molecular orbitals (MOs; Figures 5c,d; see also Figure S2), we can conclude that both HOMO-1 and LUMO + 1 exhibit a  $\pi$ -type antibonding orbital, the two of which are located at two sides of this macrocycle rather than at the equator. The energy gap between HOMO and LUMO is 1.81 eV, thus suggesting that

this structure is quite stable. Furthermore, the strain energy of [4]CHBC was calculated to be 49.18 kcal mol<sup>-1</sup> according to the reported method (see Table S1 in the Supporting Information).<sup>[22]</sup> This value is comparable to that of [12]CPP (55 kcal mol<sup>-1</sup>).<sup>[23]</sup>

Considering the concave cavity of [4]CHBC, it should act as a host for  $\pi$ -conjugated molecules with a convex surface, such as fullerenes. We next investigated the supramolecular host–guest interaction behavior between [4]CHBC and fullerene  $\text{C}_{70}$ . Their interaction was first observed when  $\text{C}_{70}$  was added to a solution of [4]CHBC in dichloromethane, whereupon the solution underwent a clear color change from yellow to brown. Accordingly, there was reduced fluorescence intensity under UV light at 365 nm. This complexation between [4]CHBC and  $\text{C}_{70}$  was then confirmed by MS

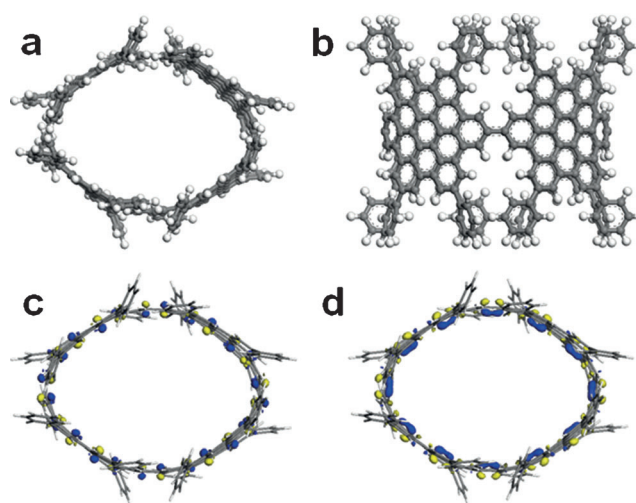


**Figure 5.** Optimized geometry and frontier MOs of [4]CHBC: a) Top view of the molecular structure; b) side view of the molecular structure; c) HOMO of [4]CHBC; d) LUMO of [4]CHBC.

spectrometry. The peak observed at  $m/z$  4814.85 (calculated for  $C_{382}H_{225} [C_{70} \subset M + H]^+$ : 4814.77; Figure 6a) suggests the formation of a 1:1 complex. We next carried out fluorescence measurements with an excitation wavelength at 400 nm. The

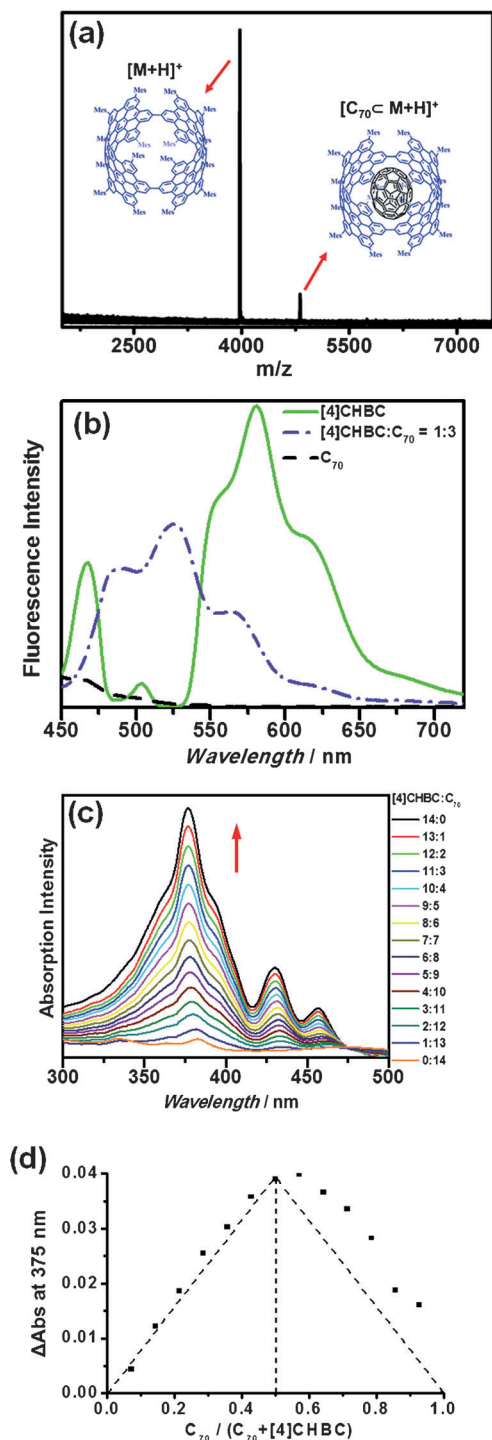


**Figure 6.** a) Mass spectrometry data for the  $C_{70} \subset [4]CHBC$  complex. b) Fluorescence spectra of [4]CHBC ( $1.11 \times 10^{-6} \text{ mol L}^{-1}$ ) in the presence of  $C_{70}$  in toluene. The concentrations of  $C_{70}$  used were  $0.00$ – $3.33 \times 10^{-6} \text{ mol L}^{-1}$ ; 3 of 17 lines are shown for simplification (see Figure S3 for all lines). c) UV/Vis spectra of [4]CHBC and  $C_{70}$  at different ratios in toluene for Job plot analysis. d) Job plot of [4]CHBC and  $C_{70}$ .

main emission peaks (554, 586, and 617 nm) showed a significant blueshift as compared with pure [4]CHBC, and the emission intensity decreased upon the addition of  $C_{70}$  to the solution of [4]CHBC in toluene at  $25^\circ\text{C}$  (Figure 6b; see also Figure S3a). On the basis of the quenching results, the binding constant ( $K_a$ ) in toluene was estimated to be approximately  $1.07 \times 10^6 \text{ M}^{-1}$  (see Figure S3b). The 1:1 complexation between [4]CHBC and  $C_{70}$  was also suggested by a UV/Vis titration experiment (Figure 6c). A Job plot of the UV/Vis spectra at 375 nm in toluene showed a maximum absorption change when the ratio of [4]CHBC and  $C_{70}$  reached approximately 1:1 (Figure 6d). We also tried to use  $C_{60}$  as the guest to investigate the supramolecular properties of [4]CHBC, but no obvious change was observed in the photophysical experiments (see Figure S4), possibly because the sizes of [4]CHBC and  $C_{60}$  are incompatible (see Figure S5).

In conclusion, the large  $\pi$ -extended molecular carbon nanoring [4]CHBC was synthesized by a platinum-mediated reductive-elimination reaction. The electronic absorption and fluorescent behavior of [4]CHBC revealed its unique optoelectronic properties. Furthermore, the tentative investigation of its interaction with  $C_{70}$  showed that a 1:1 complex can be formed. [4]CHBC would be useful for the bottom-up synthesis of structurally uniform carbon nanotubes. Further challenges, including the design and synthesis of highly conjugated carbon nanorings more similar to long CNT segments and the production of size-specific CNTs are subjects of research currently in progress in our laboratory.

### Acknowledgements

This research was supported financially by the National Natural Science Foundation of China (21271166, 21473170), the Fundamental Research Funds for Central Universities (WK2060140015, WK2060190026, WK3430000001), and the Program for New Century Excellent Talents in University (NCET).

**Keywords:** carbon nanorings · carbon nanotubes · fullerenes · host–guest systems ·  $\pi$  conjugation

- [1] J. R. Sanchez-Valencia, T. Dienel, O. Gröning, I. Shorubalko, A. Mueller, M. Jansen, K. Amsharov, P. Ruffieux, R. Fasel, *Nature* **2014**, *512*, 61.
- [2] F. Yang, X. Wang, D. Zhang, J. Yang, D. Luo, Z. Xu, J. Wei, J. Q. Wang, Z. Xu, F. Peng, X. Li, R. Li, Y. Li, M. Li, X. Bai, F. Ding, Y. Li, *Nature* **2014**, *510*, 522.
- [3] H. Omachi, T. Nakayama, E. Takahashi, Y. Segawa, K. Itami, *Nat. Chem.* **2013**, *5*, 572.
- [4] a) H. Omachi, Y. Segawa, K. Itami, *Acc. Chem. Res.* **2012**, *45*, 1378; b) B. D. Steinberg, L. T. Scott, *Angew. Chem. Int. Ed.* **2009**, *48*, 5400; *Angew. Chem.* **2009**, *121*, 5504.
- [5] V. C. Parekh, P. C. Guha, *J. Indian Chem. Soc.* **1934**, *11*, 95.
- [6] R. Friederich, M. Nieger, F. Vögtle, *Chem. Ber.* **1993**, *126*, 1723.
- [7] S. Kammermeier, P. G. Jones, R. Herges, *Angew. Chem. Int. Ed. Engl.* **1996**, *35*, 2669; *Angew. Chem.* **1996**, *108*, 2834.



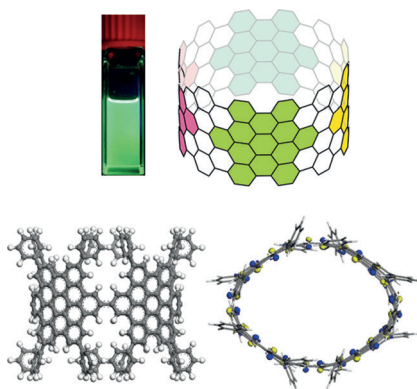
## Communications



## Host–Guest Systems

D. Lu, G. Zhuang, H. Wu, S. Wang,  
S. Yang, P. Du\* ————— ■■■■–■■■■

A Large  $\pi$ -Extended Carbon Nanoring Based on Nanographene Units: Bottom-Up Synthesis, Photophysical Properties, and Selective Complexation with Fullerene C<sub>70</sub>



A decent slice of a carbon nanotube was synthesized in the form of a large  $\pi$ -extended carbon nanoring based only on hexa-*peri*-hexabenzocoronene units (see picture). The photophysical properties of the nanoring were investigated by both steady-state and time-resolved fluorescence spectroscopy, and a selective supramolecular host–guest interaction with C<sub>70</sub> was identified.